Thermodynamic analysis of a solar-driven high-temperature steam electrolyzer for clean hydrogen production

Wei He, Mohammad Mostafa Namar, Zhixiong Li, Akbar Maleki, Iskander Tlili, Mostafa Safdari Shadloo

2020

Thermodynamic analysis of a solar-driven high-temperature steam electrolyzer for clean hydrogen production

Wei He

Mohammad Namar

Zhixiong Li
University of Wollongong, lizhixio@uow.edu.au

Akbar Maleki

Iskander Tlili

See next page for additional authors

Thermodynamic analysis of a solar-driven high-temperature steam electrolyzer for clean hydrogen production

Abstract

2020 Elsevier Ltd Increasing world population and consequent increase in fossil fuels consumption emerge the necessity of looking for new sources of energy; resources that are clean, cheap, and renewable. Hydrogen is known as a clean and renewable fuel in various approaches; so, finding clean ways of hydrogen production can be considered as an appropriate solution for climate changes and global warming. In this study, a conceptual design of solar-driven high-temperature steam electrolyzer system is presented, and its performance is investigated thermodynamically using a real-time simulator in-house code. Evaluation of the effects of inlet parameters on the system performance is performed and the system real-time performance is calculated on design day at two different sites. Results show that the proposed system is able to separate 98% of existed hydrogen in the feed water and produce pure hydrogen with the rate of 1.2 g/s with overall energy and exergy efficiencies of 21.5% and 22.5% respectively. In addition, the main exergy destructor item is reported as the solar collector with 36.4% exergy degradation of inlet exergy. Based on the results, it was deduced that the most effective parameters on heat absorption are direct normal irradiance and incidence angle while relative humidity has no major effect. Furthermore, the designed system produced 52.43kg and 26.45kg hydrogen on the design day at Sterling and Babol Noshirvani University of Technology sites. The mean annual hydrogen production for these sites were estimated 4.98 and 3.93 tons, respectively.

Disciplines

Engineering | Science and Technology Studies

Publication Details

He, W., Namar, M., Li, Z., Maleki, A., Tlili, I. & Safdari, M. (2020). Thermodynamic analysis of a solar-driven high-temperature steam electrolyzer for clean hydrogen production. Applied Thermal Engineering, 172

Authors

Wei He, Mohammad Namar, Zhixiong Li, Akbar Maleki, Iskander Tlili, and Mostafa Safdari

Thermodynamic analysis of a solar-driven high-temperature steam electrolyzer for clean hydrogen production

Wei He
Engineering Research Center of Fujian University for Marine Intelligent Ship Equipment, Minjiang University, Fuzhou 350108, China
E-mail: hewei.mju@gmail.com

Mohammad Mostafa Namar
Faculty of Mechanical Engineering, Babol Noshirvani University of Technology, Babol, Iran, E-mail: m.namar@stu.nit.ac.ir

Zhixiong Li
Engineering Research Center of Fujian University for Marine Intelligent Ship Equipment, Minjiang University, Fuzhou 350108, China.
School of Mechanical, Materials, Mechatronic and Biomedical Engineering, University of Wollongong, NSW 2522, Australia
E-mail: lzx___520@163.com

Akbar Maleki
Faculty of Mechanical Engineering, Shahrood University of Technology, Shahrood, Iran
E-mail: a_maleki@shahroodut.ac.ir

Iskander Tlili[1]
Department for Management of Science and Technology Development, Ton Duc Thang University, Ho Chi Minh City, Vietnam
Faculty of Applied Sciences, Ton Duc Thang University, Ho Chi Minh City, Vietnam
E-mail: iskander.tlili@tdtu.edu.vn

Mostafa Safdari Shadloo
Associate Professor, CORIA Lab./CNRS, University and INSA of Rouen, Normandie University, 76000 Rouen, France
E-mail: msshadloo@coria.fr

Abstract:

Increasing world population and consequent increase in fossil fuels consumption emerge the necessity of looking for new sources of energy; resources that are clean, cheap, and renewable. Hydrogen is known as a clean and renewable fuel in various approaches; so, finding clean ways of hydrogen production can be considered as an appropriate solution for climate changes and global warming. In this study, a conceptual design of solar-driven high-temperature steam

[1] Corresponding Author Email: Iskander Tlili (Email: iskander.tlili@tdtu.edu.vn)

electrolyzer system is presented, and its performance is investigated thermodynamically using a real-time simulator in-house code. Evaluation of the effects of inlet parameters on the system performance is performed and the system real-time performance is calculated on design day at two different sites. Results show that the proposed system is able to separate 98% of existed hydrogen in the feed water and produce pure hydrogen with the rate of $1.2 g/s$ with overall energy and exergy efficiencies of 21.5% and 22.5% respectively. In addition, the main exergy destructor item is reported as the solar collector with 36.4% exergy degradation of inlet exergy. Based on the results, it was deduced that the most effective parameters on heat absorption are direct normal irradiance and incidence angle while relative humidity has no major effect. Furthermore, the designed system produced $52.43 kg$ and $26.45 kg$ hydrogen on the design day at Sterling and Babol Noshirvani University of Technology sites. The mean annual hydrogen production for these sites were estimated 4.98 and 3.93 tons, respectively.

Keywords: Conceptual design, Thermodynamic analysis, Solar driven HTSE, Hydrogen, Clean production.

1. Introduction

The importance of energy and its crisis worldwide has been increasingly noticed during the recent years [1]. Increasing world population and consequent increase in fossil fuels consumption emerge the necessity of looking for new sources of energy; resources that are clean, cheap, and renewable [2]. Accordingly, the use of renewable energy resources such as those in hydrogen, fuel cell [3-5], wave [6, 7], tidal [8], wind [9], solar [10], geothermal [11, 12] and, hydrothermal energies are gained considerable attention. In many industrial applications, the combination of the above resources are applied [13-16]. In addition to becoming a competitive source of energy in terms of production cost, they are environmentally friendly, i.e., greenhouse gas emissions as the most

critical factors on global warming are negligible, and are accessible in remote regions [17]. Recently, hydrogen has been considered and evaluated in a wide range of research as both additive and pure fuel [18, 19] to feed material of ammonia production [20] as a clean and alternative renewable energy resource. The pure hydrogen is not available on Earth while it is widely found in composition with other materials. So, hydrogen extraction is considered as one of the noticed fields of studies and therefore, numerous research is executed [21-28].

The different methods of hydrogen production [29-32] are investigated in detail in the literature and briefly are reported in Table 1; high-temperature steam electrolysis (HTSE) is considered as one of the cheapest methods besides having acceptable performance. In this method, feed water is superheated first using different energy resources such as solar [33], wind [34], nuclear [35], and geothermal [36-39]. Then, superheated steam breaks down to pure hydrogen and oxygen by applying electricity in electrolyzer. This method is generally more efficient compared to low-temperature method due to better ionic conduction [40, 41].

Table 1: Different methods of hydrogen production [42]

Method		**Normalized cost**	**Normalized energy efficiency**
Electrolysis	Low temperature	7.34	5.30
	High temperature	5.54	2.9
	Photovoltaic	4.50	1.24
Photoelectrolysis		7.09	0.78
Photocatalysis		5.19	0.20
Biophotolysis		7.27	1.40
Photoelectrochemical method		0.00	7.00
Photofermentation		7.61	1.50
Artificial photosynthesis		7.54	0.9
Thermolysis		6.12	5.00
Thermochemical water splitting		8.06	4.20
Hybrid thermochemical cycles		7.41	5.30
Biomass conversion		8.10	5.60
Gasification	Biomass	8.25	6.50
	Coal	9.11	6.30
Reforming	Biomass	7.93	3.90
	Fossil fuel	9.28	8.30
Plasma arc decomposition		9.18	7.00
Dark fermentation		7.52	1.30
Base (zero emission, zero cost, 100% efficiency)		10.00	10.00

Zhang et al. studied a solar-driven HTSE system for hydrogen production [43]. In their research, the main energy consumption processes including steam electrolysis, heat transfer, and product compression processes were considered. The detailed thermodynamic-electrochemical modeling of the solid oxide steam electrolysis was implemented, and subsequently, the electrical and thermal energy required by every energy consumption process were determined. Mingyi et al. investigated the calculation of overall efficiency of a HTSE by electrochemical and thermodynamic analysis [44]. They established a thermodynamic model in regards to the efficiency of the HTSE system the quantitative effects of three key parameters, electrical efficiency, electrolysis efficiency, and thermal efficiency on the overall efficiency of the HTSE system were studied. Based on their results, the contribution of electrical efficiency, electrolysis efficiency, and thermal efficiency to the overall efficiency were about 70%, 22%, and 8%, respectively. Herring et al. [45] performed numerical and experimental analyses of a high temperature solid oxide steam electrolysis, and demonstrated 90 NL/hr of production rate. They performed a parametric study to investigate the performance of the electrolyzer at different temperatures, steam inlet mole fractions, gas flow rates and current densities.

Although extensive research has been done on HTSEs to improve their performance, more studies are still needed to find sustainable, high performance and environmentally friendly methods. The range of proposed methods in the literature are widely extended from employing different renewable energy resource [46, 47] to applying thermodynamic investigations [48, 49] and using numerical optimizations [49-52]. Kim et al. [46] proposed a greenhouse gas-free HTSE system by employing nuclear-renewable hybrid energy system which is capable of supplying grid power as well as HTSE on an industrial scale. Yadav and Banerjee [47] employed solar energy for their proposed HTSE with two different modes, namely, concentrated solar and photovoltaic power

plants. Enhancement of energy efficiency from 9.1 to 12.1% by operating temperature shifting between 873 and 1273 K was reported in this study. Kaleibari et al. [48] were numerically modelled a solar-driven HTSE system integrated with solar tower and concentrated photovoltaic. They asserted that their provided system has 36.5% energy efficiency and produce 850 g/h hydrogen with 899 W/m^2 direct normal irradiance (DNI). Nafchi et al. [49] explored a solar hydrogen and electricity production plant by a finite-time-thermodynamic analysis and claimed that the energy and exergy efficiencies of the integrated system (hydrogen plus electricity generation) were 20.1% and 41.25%, respectively. A multi-objective genetic algorithm was used for the optimization of a proton exchange membrane electrolyzer performance by Habibollahzade et al. [53]; the exergy efficiency and total product cost at the optimum point of their system are reported 63.96% and 13.29 $\$/GJ$, respectively.

In the present study, a solar-driven HTSE system is designed and analyzed thermodynamically to reduce the emission of this type of system previously designed by other researchers. A solar-driven Rankine cycle is replaced as the power generation section and also demanded heat of superheated steam generation are provided by the parabolic solar concentrator. The thermodynamic model, real-time simulator in-house code, of the proposed system is used for the designing process, parametric study, and also case studies. Designed system real-time performance is investigated at design day in two sites, namely Sterling, Virginia, USA, and Babol Noshirvani University of Technology (NIT), Babol, Iran.

2. System Description

The schematic of the designed system is shown in Fig.1. In this figure, a solar-driven Rankine cycle is applied to provide the demanded power of the electrolyzer. The parabolic solar concentrator is used to absorb solar energy. The power required to run the Rankine cycle and the

HTSE is supplied by the oil flow between the collector and the storage tank. In the Rankine cycle, pressure of saturated water from condenser's outlet is increased up to open feedwater heater (OFWH) working pressure, and it is re-pumped to high pressure (HP) of the designed cycle after re-heating with extracted steam from low pressure (LP) turbine. Achieved compressed liquid is then converted to superheat steam with fixed-designed temperature in the boiler and this high energy steam runs the HP turbine. The steam loses its energy passing the HP turbine blades, so it is re-heated to cycle high temperature and then enters the LP turbine. Designed pressure of re-heating at the boiler is assumed to be geometrical mean of cycle HP and LP ($\sqrt{P_6 P_9}$). Also for open water supply, this pressure (operating pressure) is determined based on obtaining the best energy and exergy performances as shown in Fig. 2. The high performance electrolyzer section is adapted from [54] which has 98% hydrogen separation efficiency. The inlet mass flow rate of electroyzer is determined considering the absorbed heat in solar collector which should be able to provide the demanded temperature of electrolyzer entrance steam after supplying the boiler needed heat. The characteristics of the above mentioned sections are described in Table 2.

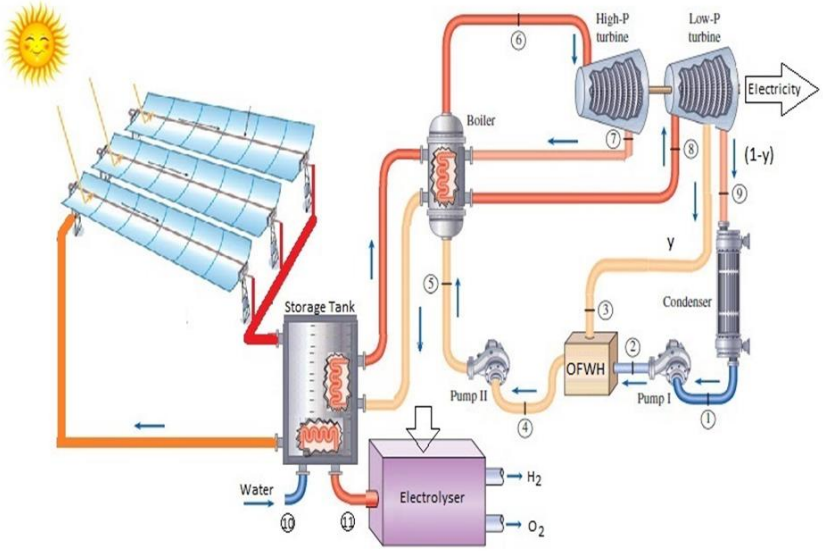

Figure 1: The schematic of the designed system

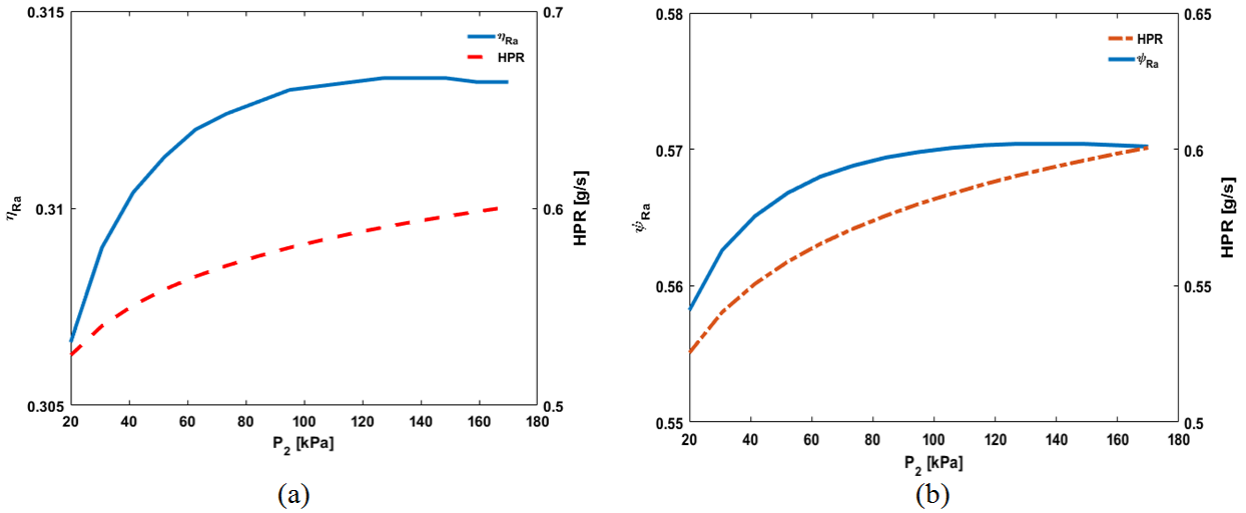

Figure 2: System performance variations in terms of (a) energy and (b) exergy with changing the OFWH operating pressure

Table2: The characteristics of each section

Solar collector [55]	
Area	1000 m^2
Optical efficiency	73.3 %
Absorber number of rows * length	5*100 m
Absorber pipe inner, outer diameters	0.066, 0.07 m
Glass tube diameter	0.115 m
Rankine cycle	
Mass flow rate	0.1 kg/s
Condenser, boiler pressures	10, 3000 kPa
Boiler out temperature	623 K
Pumps and turbines isentropic efficiency	90 %
Electrolyzer [54]	
Inlet steam temperature	725 K
Electrolyzer temperature	1233 K
Hydrogen separation efficiency	98 %

3. Modeling

The process of each device used in the system is examined by applying the first and second laws of thermodynamics on that device as a control volume (CV). In this section, the governing equations are described in detail, and the following assumptions are considered for the simulation:

- All devices are assumed to have Steady-State Steady Flow (SSSF).

- The outflows from the condenser and OFWH are considered as a saturated liquid.
- The pressure losses of connecting pipes are ignored.
- The outlet temperature of the boiler is constant, and it is equal to the maximum temperature of the Rankine cycle.
- The storage tank design temperature is set at 30 K above the maximum Rankine cycle temperature in order to operate the system.

3.1. Solar Collector

The characteristics of parabolic solar concentrator is explained by Odeh et al. [55] in which the collector efficiency, absorbed heat flux rate relative to incoming heat flux rate, was defined as the function of collector optical efficiency (η_{opt}), direct normal irradiance, incident angle modifier ($k_{\tau\alpha}$), wind speed (V_{wind}), emissivity of the cermet selective coating (ε_{ab}) and the temperatures of absorber pipe (T_{ab}), sky (T_{sky}) and ambient (T_{amb}).

$$\eta_{Collector} = \eta_{opt}\, k_{\tau\alpha} - (a + c\, V_{wind}) \frac{T_{ab} - T_{amb}}{DNI} - \varepsilon_{ab}\, b\, \frac{T_{ab}^4 - T_{sky}^4}{DNI} \quad (1)$$

Where, a, b and c are considered 1.91e-02 $WK^{-1}m^2$, 2.02e-09 $WK^{-4}m^{-2}$ and 6.608e-03 $JK^{-1}m^3$, respectively which were achieved from thermal analysis of the collector. The schematic of various losses for solar heat absorption are shown in Fig. 3.

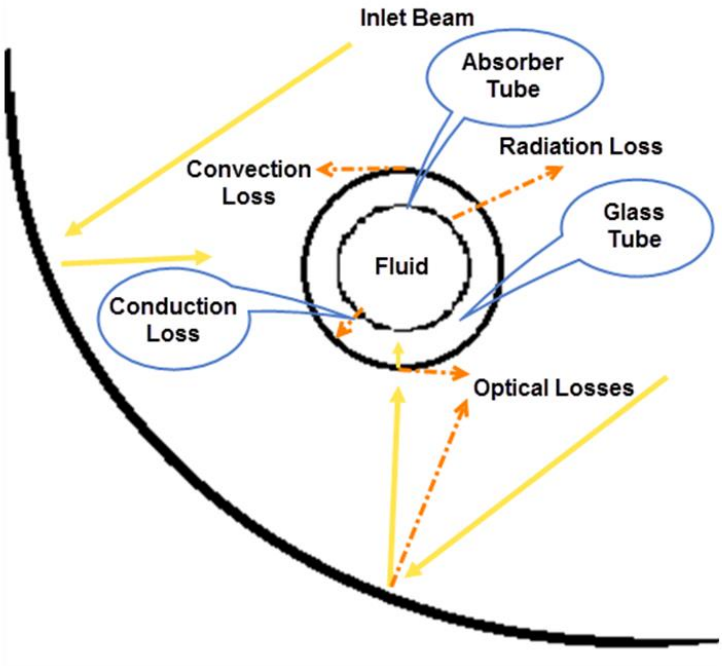

Figure 3: The schematic of various losses for solar heat absorption

The incident angle modifier and also emissivity of the cermet selective coating were determined by Dudley et al. [56] as,

$$k_{\tau\alpha} = \cos(\theta) + 9.94 * 10^{-4}\,\theta - 5.369 * 10^{-5}\,\theta^2 \quad (2)$$

$$\varepsilon_{ab} = 4.2 * 10^{-4}\,T_{ab} - 9.95 * 10^{-2} \quad (3)$$

Where, θ refers to the angle between the inlet beam incidence and the normal vector of collector surface. The sky temperature was also defined by Martin and Berdahl [57] as the function of the dew point (T_{dp}),

$$T_{sky} = \varepsilon_{sky}^{0.25}\,T_{amb} \quad (4)$$

$$\varepsilon_{sky} = 0.711 + 0.56\,(T_{dp}/100) + 0.73\,(T_{dp}/100)^2 \quad (5)$$

3.2. Rankine cycle

The mass conservation, energy, and exergy equations of multi-inputs-multi-outputs CV at SSSF condition can be written as [58],

$$\sum \dot{m}_i = \sum \dot{m}_e \tag{6}$$

$$\dot{Q} - \dot{W} = \sum \dot{m}_e\, h_e - \sum \dot{m}_i\, h_i \tag{7}$$

$$\dot{Ex}^{Q} + \sum \dot{m}_i\, ex_i = \dot{Ex}^{W} + \sum \dot{m}_e\, ex_e + I \tag{8}$$

Where $\dot{m}$, h, ex and I are the mass flow rate, specific enthalpy, specific exergy and exergy destruction rate, respectively. Subscripts i and e refer to inlet and exhaust flows. Ignoring the chemical term of exergy, the specific exergy of each stream can be considered equal to the thermo-mechanical exergy,

$$ex = (h - h_0) - T_0(s - s_0) \tag{9}$$

Here, s and T are the specific entropy and temperature and subscript 0 refers to the dead state which is defined as the condition of fluid at ambient pressure and temperature. The exergy transferred by heat ($\dot{Ex}^{Q}$) and work could be written as:

$$\dot{Ex}^{Q} = \dot{Q}\,(1 - \frac{T_{amb}}{T_s}) \tag{10}$$

$$\dot{Ex}^{W} = \dot{W} \tag{11}$$

Where, T_s is the temperature of the heat source. Turbine and pump isentropic efficiencies can be defined as:

$$\eta_{tur} = \frac{h_i - h_e}{h_i - h_{es}} \tag{12}$$

$$\eta_{pump} = \frac{h_i - h_{es}}{h_i - h_e} \tag{13}$$

Here, subscript es indicates that the calculations are based on isentropic operation.

3.3. Electrolyzer

Liquid water is converted to the superheated steam in an isobar heating process, and then with employing the supplied electricity from Rankine cycle, the superheated steam is decomposed to hydrogen and oxygen applying the high temperature electrolyze method [59]. Energy equation of steam electrolyze reaction can be written as:

$$H_2O + Energy \longrightarrow H_2 + \frac{1}{2}O_2 \tag{14}$$

$$Energy = Q + W = \sum n_P \left(\overline{h_f^0} + \bar{h} - \overline{h^0}\right)_P - \sum n_R \left(\overline{h_f^0} + \bar{h} - \overline{h^0}\right)_R \tag{15}$$

Where n refers to the number of moles and $\overline{h_f^0}$ is the molar enthalpy of formation. The subscripts P and R refer to the reaction products and reactants, respectively. The terms of enthalpy values for each species are calculated by Shomate equation [60]:

$$\bar{h} - \overline{h^0} = A\,T + B\frac{T^2}{2} + C\frac{T^3}{3} + D\frac{T^4}{4} + E\frac{1}{T} + F - H \tag{16}$$

Here, T is the specified temperature in 1/1000 Kelvin, and the Shomate constant of each species are reported in Table 3. Separated hydrogen mass flow rate can be obtained by;

$$\dot{m}_{out,H_2} = (1 - r)\,\dot{m}_{H_2O}\frac{M_{H_2}}{M_{H_2O}} + r\,\dot{m}_{H_2O} \tag{17}$$

Where r is the recycling ratio which is considered 0.02 from ref [54] and M is the molecular weight of species.

Table 3: The enthalpy of formation and Shomate constant of each species [61]

Species	$\overline{h_f^0}$ $(\frac{\boldsymbol{kJ}}{\boldsymbol{kmol}})$	**A**	**B**	**C**	**D**	**E**	**F**	**G**	**H**
$H_2O\ (g)$	-241830	30.0920	6.832514	6.793435	-2.534480	0.082139	-250.881	223.3967	-241.8264
$O_2(g)$	0	29.6590	6.137261	-1.186521	0.095780	-0.219663	-9.861391	237.9480	0
$H_2(g)$	0	33.0661	-11.36340	11.432816	-2.772874	-0.158558	-9.980797	172.7079	0

3.4. General Analyzing

In this study, the results are reported on two basis. First, the sun's incoming beams are considered as the input energy and is called as overall, and the second is the energy absorbed in the collector which is considered as an input for calculations, and is called as total. The equations that are used for calculations of this study are reported in Table 4.

Table 4: The used calculations of this study

Name	Equations
Solar collector	
Inlet heat rate (kW)	$\dot{Q}_{in} = DNI * A_{collector}/1000$
Collector efficiency	$\eta_{Collector} = \dot{Q}_{abs}/\dot{Q}_{in}$
Inlet exergy rate (kW) [62]	$\dot{E}x_{in} = \frac{DNI}{1000} * A_{collector}\left(1 + \frac{1}{3}\left(\frac{T_0}{T_{sun}}\right)^4 - \frac{4}{3}\frac{T_0}{T_{sun}}\right)$
Rankine cycle	
Net power (kW)	$\dot{W}_{net} = \dot{W}_{LP\ Turbine} + \dot{W}_{HP\ Turbine} + \dot{W}_{Pump1} + \dot{W}_{Pump2}$
First law efficiency	$\eta_{Ra} = \dot{W}_{net}/\dot{Q}_{Boiler}$
Second law efficiency	$\psi_{Ra} = \dot{W}_{net}/\dot{Q}_{Boiler}\left(1 - \frac{T_0}{T_{ab}}\right)$
Electrolyzer	
First law efficiency	$\eta_{Total} = \frac{\dot{m}_{out,H_2} HHV_{H_2}}{\dot{Q}_{abs}}$ $\eta_{Overall} = \frac{\dot{m}_{out,H_2} HHV_{H_2}}{\dot{Q}_{in}}$
Second law efficiency	$\psi_{Total} = \frac{\dot{m}_{out,H_2} ex_{H_2}}{\dot{Q}_{abs}\left(1 - \frac{T_0}{T_{ab}}\right)}$ $\psi_{Overall} = \frac{\dot{m}_{out,H_2} ex_{H_2}}{\dot{E}x_{in}}$

4. Results and Discussion:

A thermodynamic model of the proposed system has created considering the abovementioned equations to estimate the performance of the overall system and also to investigate each part of the

system independently. The solar farm and electrolyzer sections are adopted and validated in the previous works [54, 55] while the Rankine cycle is designed conceptually to analyze the system feasibility. The thermodynamic characteristics of each defined stream and also the general system performance are reported in Table 5. The simulation results show that the proposed system is able to separate 98% of existed hydrogen in feed water and produce pure hydrogen with the rate of $1.2 g/s$. Also, the solar collectors are able to produce $632 K$-superheated steam absorbing the 64.4% of inlet beams energy. Given the Rankin cycle power output rate of 101 kW, the energy efficiency (first law) for the proposed system is calculated 33.4% considering the absorbed heat in collectors as input energy and it is equal to 21.5% with considering the incoming radiation as input energy.

Table 5: Each stream characteristics and general performance of the proposed system

State	Fluid	$P\ [kPa]$	$T\ [K]$	$h\ [kj/kg]$	$s\ [kj/kgK]$	$ex\ [kj/kg]$
Dead	Water	101	293	83.3	0.294	0
1	Water	10	318.9	191.7	0.6489	4.446
2	Water	150	318.9	191.9	0.6489	4.588
3	steam	150	604.9	3137	8.136	756.1
4	Water	150	384.5	467.1	1.433	49.91
5	Water	3000	384.8	470.4	1.434	52.99
6	Steam	3000	623	3114	6.741	1142
7	Steam	173.2	388.9	2589	6.891	573.1
8	steam	173.2	623	3174	8.129	794.6
9	steam	10	346.9	2637	8.308	205.5
10	Water	101	293	83.3	0.294	0
11	steam	101	725	8726	12.09	5188
General performance						
Collector efficiency			64.44 %	Inlet energy		800 kW
Electrolyzer efficiency			98 %	Inlet exergy		745.9 kW
Total energy efficiency			33.44 %	Absorbed energy		515.5 kW
Total exergy efficiency			59.42 %	Rankine energy efficiency		31.33 %
Overall energy efficiency			21.55 %	Rankine exergy efficiency		57.04 %
Overall exergy efficiency			22.56 %	Rankine net power		101.1 kW
Hydrogen production rate			1.2 g/s	Rankine exergy destruction		76.17 kW

As it is mentioned in Table 5, the energy efficiency of the Rankine cycle is 31.3% and it is able to provide $101kW$ pure power. However, with $76kW$ exergy destruction, it still has 57% exergy efficiency. Boiler is reported as the main exergy destruction source of Rankine cycle with dedicating 61% of $76kW$ exergy destruction to itself and the condenser has the second rank by 24%. Both turbines have the same proportion and the pumps are the least exergy destructors devices in the Rankine cycle. These are shown with a pie chart in Fig. 4.

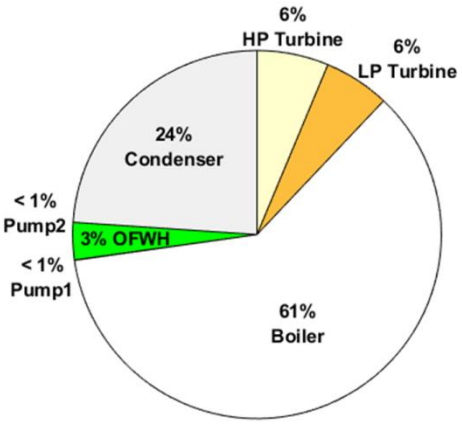

Figure 4: The proportion of each component of the Rankine cycle in Rankine net exergy destruction

The 63.6% of solar inlet exergy is absorbed by collectors, and then this high-performance exergy is shared between electrolyzer and Rankine cycle. $229kW$ and $77kW$ of absorbed exergy are destructed by electrolyzer due to optical efficiency, conduction, convection and radiation losses, and Rankine cycle, due to the heat transfer and energy conversion losses, respectively and finally, 22.5% of this exergy is achievable as pure hydrogen. The exergy flow diagram is depicted in Fig. 5.

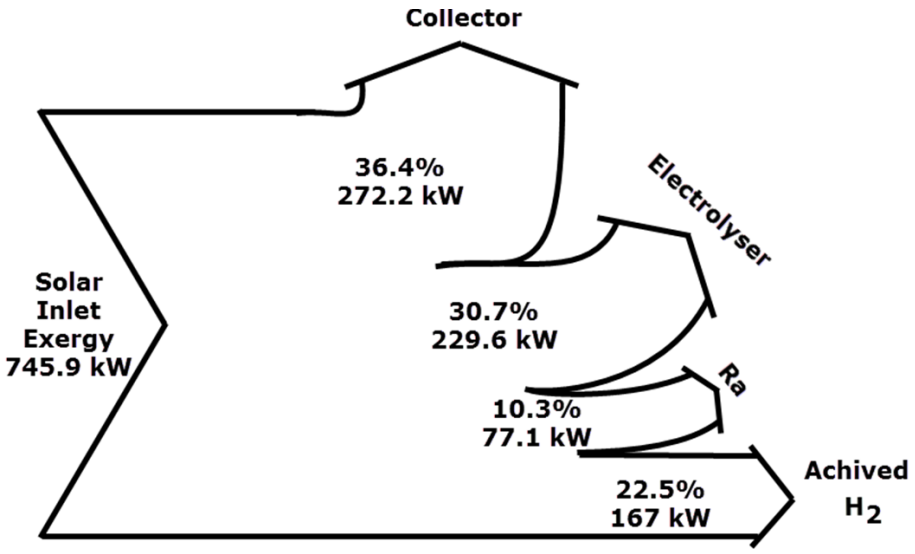

Figure 5: Exergy flow diagram

4.1 Parametric study

To study the sensitivity of overall system and its sub-systems performance to variations of inlet parameters, a parametric study is applied to the model. For achieving this purpose, each inlet parameter is varied in the applicable range besides keeping others constant. These inlet parameters are namely; DNI, incidence angle, relative humidity, and wind speed. In Fig. 6, the effect of DNI on system performance is shown. Both inlet and absorbed heat are increased linearly by DNI augmentation but with different slopes. As can be seen in this figure, the rate of collector efficiency increment is higher before DNI=800W/m^2. This trend is the same for both energy and exergy efficiencies of the overall system. However, considering the system design structure, the Rankine cycle has not benefited from extra heat caused by DNI enhancement. All extra heat is applied to electrolyzer section and hydrogen production rate is raised 3.5 times at DNI=1000W/m^2 in comparison with DNI=550W/m^2. However, more heat transfer means more irreversibility and as a result, the electrolyzer exergy destruction is increased by 2.5 times too.

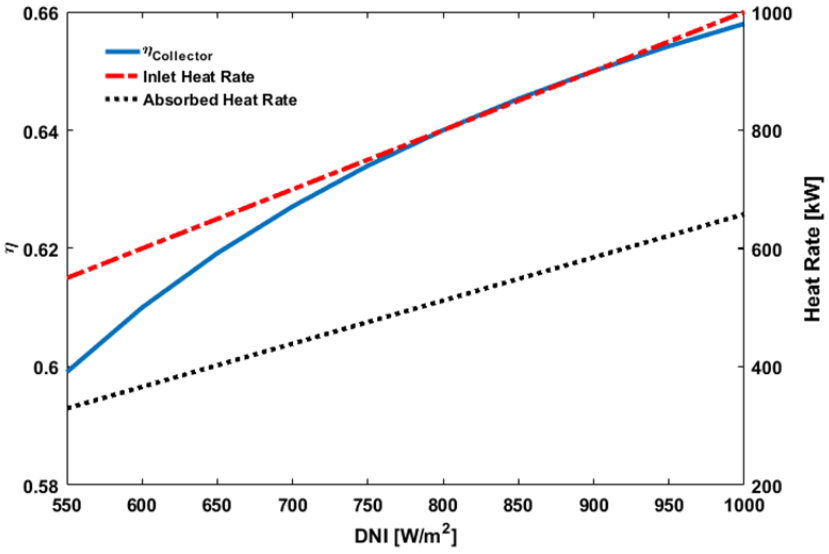
$\eta_{Collector}$
Inlet Heat Rate
Absorbed Heat Rate
η
Heat Rate [kW]
DNI [W/m^2]
0.66
0.64
0.62
0.6
0.58
1000
800
600
400
200
550
600
650
700
750
800
850
900
950
1000

(a)

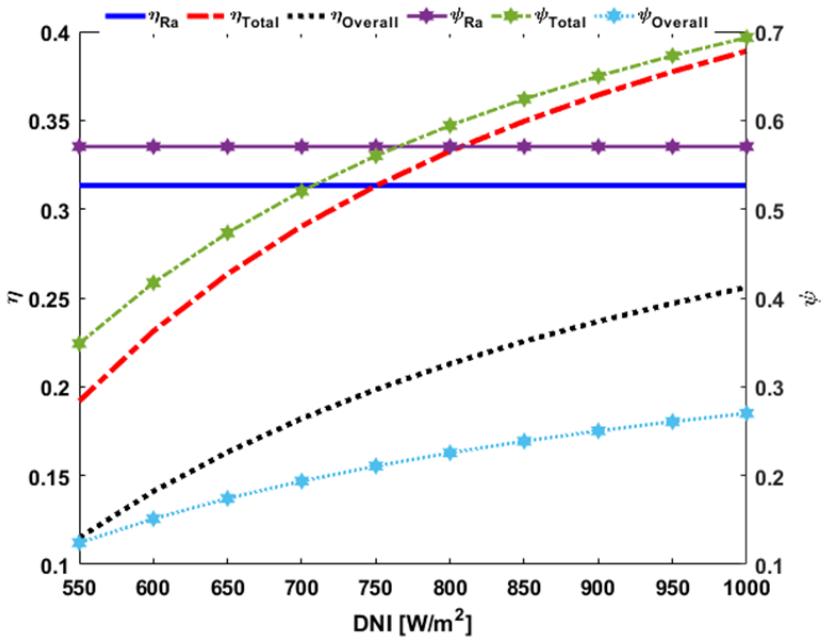
η_{Ra}
η_{Total}
$\eta_{Overall}$
ψ_{Ra}
ψ_{Total}
$\psi_{Overall}$
η
ψ
DNI [W/m^2]
0.4
0.35
0.3
0.25
0.2
0.15
0.1
0.7
0.6
0.5
0.4
0.3
0.2
0.1
550
600
650
700
750
800
850
900
950
1000

(b)

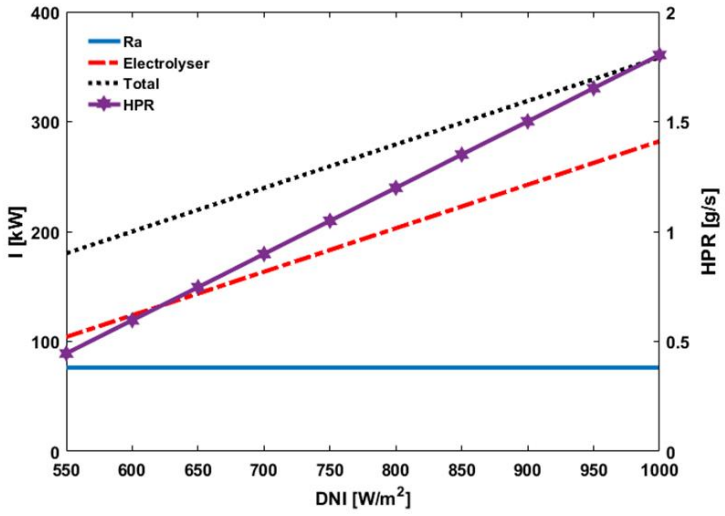

(c)

Figure 6: Variations of system performance with DNI, (a) collector (b) first and second laws efficiencies (c) exergy destruction and hydrogen production rate

In the parabolic solar collector, one of key parameters on heat absorption is the angle between the inlet beams and the normal vector of reflective surface center. The best position is the parallel form, i.e., incidence angle equals to zero, and more beams will be destructed by increasing the incidence angle. 20% reduction from 64.4% to 43.9% in collector efficiency is observed due to the incidence angle rise from 0 to 40 degrees in Fig. 7. However, the rate of heat absorption reduction before 13 degrees is much less and 2.5% reduction is detected at θ=13 degrees. This trend is the same for system energy and exergy efficiencies. Hydrogen production rate is also reduced by more than 2 times at θ=40 degrees due to the less applied heat energy to the electrolyzer. In addition, total exergy destruction is reduced by $89kW$ in this range due to the less heat transfer.

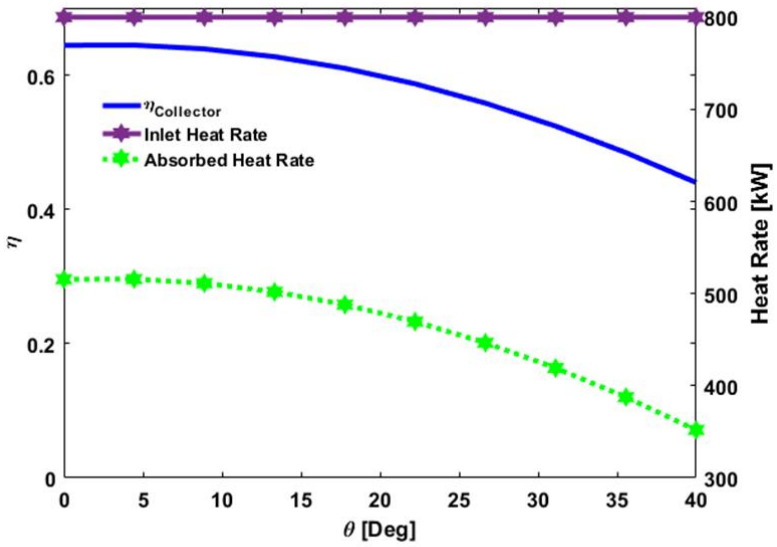
$\eta_{Collector}$
Inlet Heat Rate
Absorbed Heat Rate
η
Heat Rate [kW]
θ [Deg]

(a)

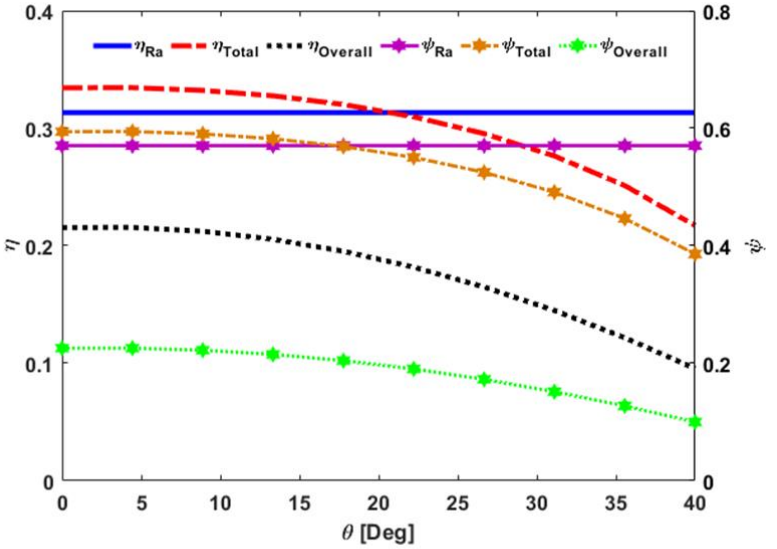
η_{Ra}
η_{Total}
$\eta_{Overall}$
ψ_{Ra}
ψ_{Total}
$\psi_{Overall}$
η
ψ
θ [Deg]

(b)

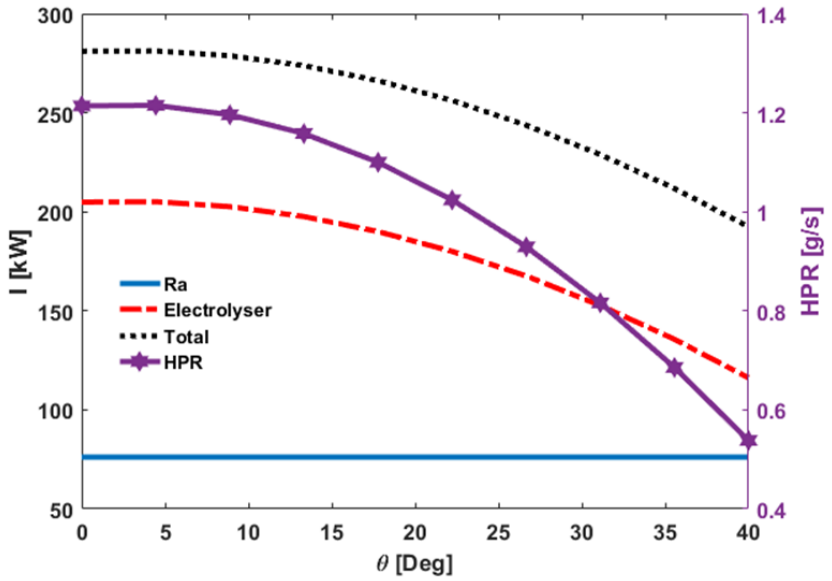

(c)

Figure 7: Variations of system performance with θ, (a) collector (b) first and second laws efficiencies (c) exergy destruction and hydrogen production rate

The relative humidity and wind speed variations are investigated in the next step; both of these parameters make a slight change on the system performance. Although both dew point and sky temperatures are increased by relative humidity enhancement, it has no significant effect on the system overall performance. In Fig. 8, hydrogen production rate is reported almost constant by altering the relative humidity. Additionally, absorbed heat and in consequence, collector efficiency are decreased by increasing the wind speed, which is shown in Fig. 9. The convection loss in absorber pipe is increased, so more exergy is destructed in this section. 0.7% and 1% reduction in overall energy and exergy efficiencies are reported by increasing the wind speed from 0 to $5m/s$ in the sections (Figs. 9-b and 9-c). Heat transferred to electrolyzer would decrease as heat absorption falls and this would lead to reduction of electrolyzer exergy destruction by 6.0 kW. In addition, hydrogen production rate is decreased by 0.05g/s.

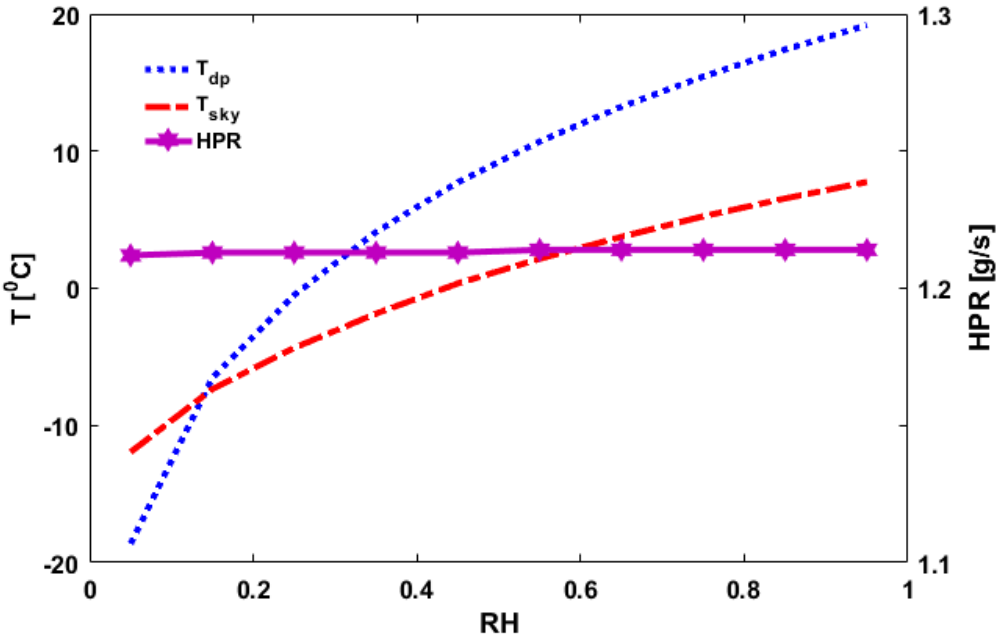

Figure 8: Hydrogen production rate, dew point, and sky temperatures variations with relative humidity

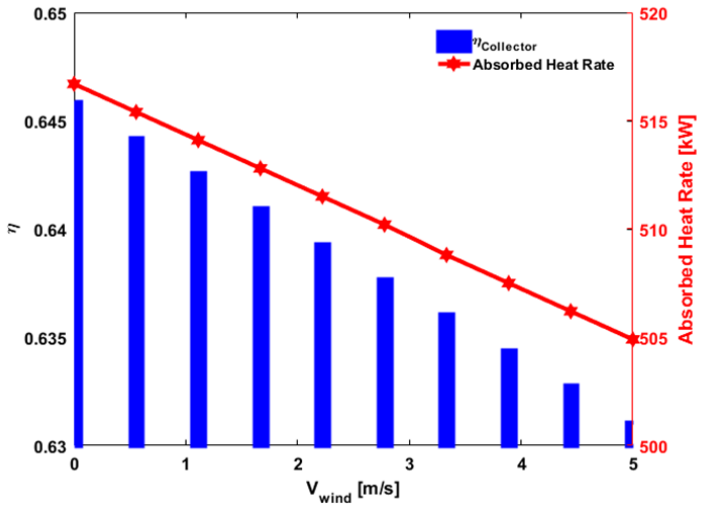

(a)

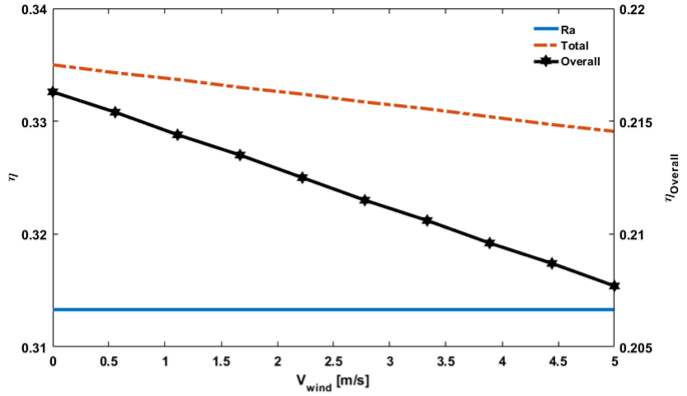

(b)

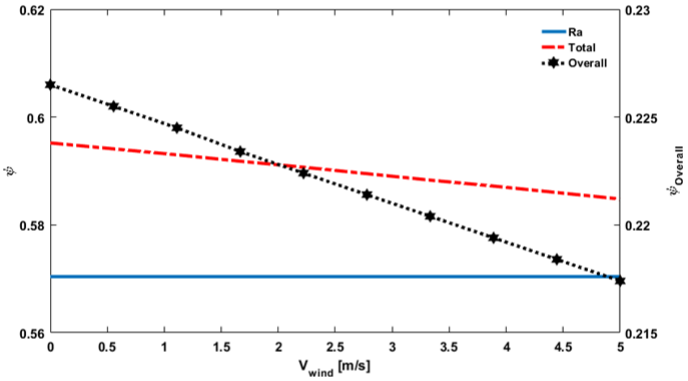

(c)

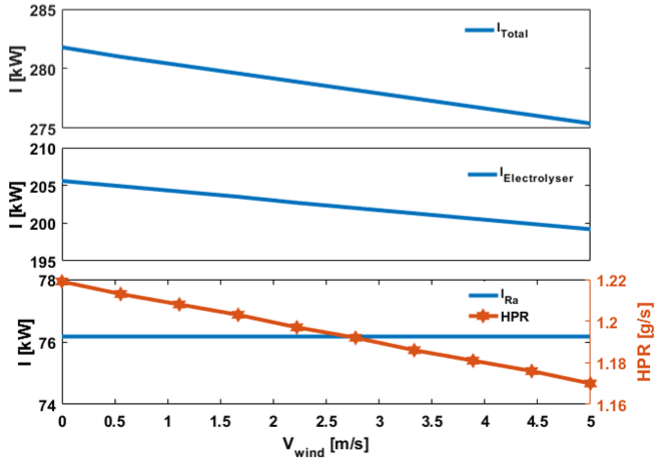

(d)

Figure 9: Variations of system performance with wind speed, (a) collector (b) first law efficiency (c) second law efficiency (d) exergy destruction and hydrogen production rate

The performance of proposed system due to the main effective parameters is investigated by Figs. 6 to 9. An implicit correlation can be defined for hydrogen production rate employing polynomial

curve fitting method for each parameter while others are given fixed and finally by using superposition assumption, a general correlation can be found [63]. The implicit correlations of hydrogen production rate due to the dependent parameters are reported in Table 6.

Table 6: The implicit correlations of hydrogen production rate due to the dependent parameters

Parameter	Implicit correlation	Initial values
DNI	$\dot{m}_{HPR} - \dot{m}_{HPR0} = 0.003034\ (DNI - DNI_0)$	$m_{HPR0} = 1.214\ , DNI_0 = 800$
Wind speed	$\dot{m}_{HPR} - \dot{m}_{HPR0} = -0.00972\ (V_{Wind} - V_{Wind0})$	$m_{HPR0} = 1.214\ , V_{Wind0} = 0.5$
Incidence angle	$\dot{m}_{HPR} - \dot{m}_{HPR0} = -0.0004737\ (\theta - \theta_0)^2 + 0.002002\ (\theta - \theta_0)$	$m_{HPR0} = 1.214\ , \theta_0 = 0.0$

Considering superposition assumption and also the similarity of initial value of hydrogen production rates in Table 6, general implicit correlation of hydrogen production rate is,

$$\dot{m}_{HPR} - \dot{m}_{HPR0} = 0.003034\ (DNI - DNI_0) - 0.00972\ (V_{Wind} - V_{Wind0}) - 0.0004737\ (\theta - \theta_0)^2 + 0.002002\ (\theta - \theta_0)$$

Where, $\dot{m}$, DNI, V_{Wind}, and θ are in g/s, $W/m\text{^}2$, m/s and deg, respectively. To consider the required accuracy, errors are plotted in Fig.10 for studied cases. Results show that the predicted hydrogen production rates are well fitted by test data with no more than 2.5% error.

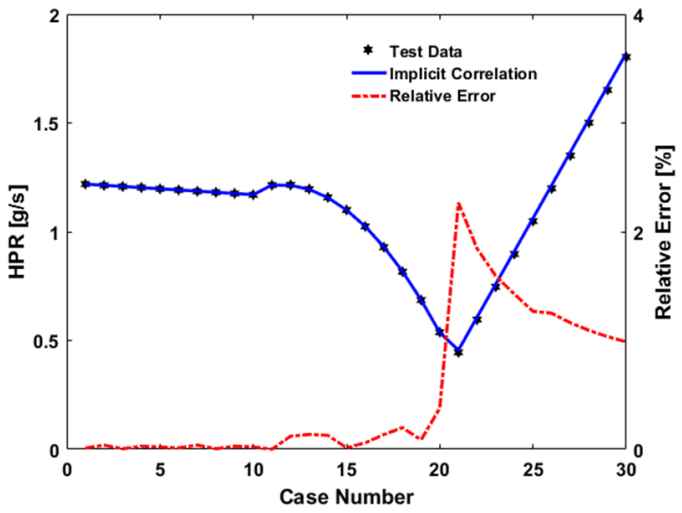

Figure 10: The error of general implicit correlation of hydrogen production rate

4.2 Case study

In the next step, to investigate the real-time operation of the designed system, its performance is explored at the date 15/June/2018, for two site locations namely; Sterling, Virginia, USA and Babol Noshirvani University of Technology (NIT), Babol, Iran. The weather variation data during this date is derived from ref [64] with two main assumptions; wind speed and ambient temperature are reported at $10m$ and $2m$ above the ground, respectively.

Case1:

Sterling, Virginia, USA, with the latitude of 38.98 and longitude of -77.47 is selected as the first location for system performance analysis. The solar data of this site is derived from ref [65], and the variations of inlet parameters during the design day are shown in Fig. 11.

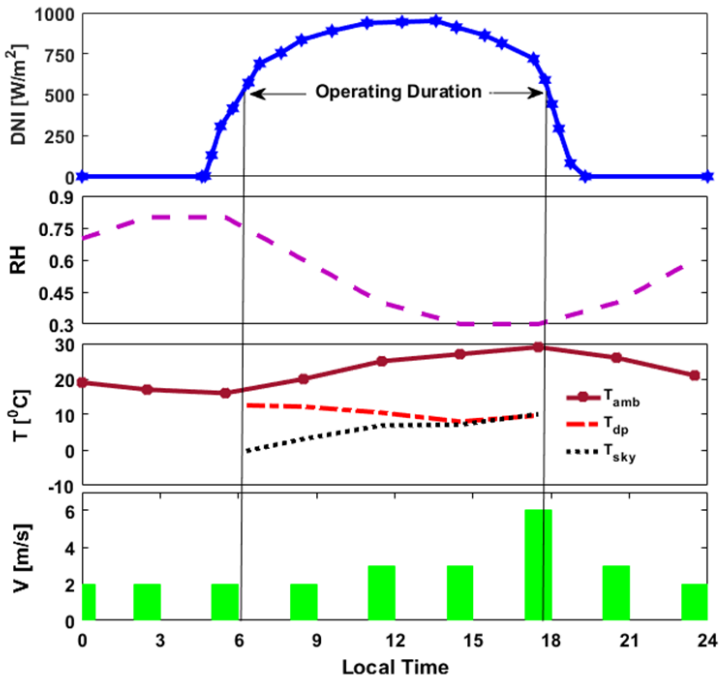

Figure 11: The variation of solar irradiance and weather condition in Sterling, Virginia, USA on 15/06/2018

As it is shown in Fig. 11, the system can be run for almost $12hr$ due to the sun radiation and during the run time, the collector efficiency has slightly changed between 60% and 65% that is shown in Fig. 12. Peak of inlet heat flux from the sun is occurred at 11:30am, local time, and hydrogen production rate is also estimated by $1.61g/s$ at the peak time which is shown in Fig. 13. In general, the potential of hydrogen production at Sterling site on design day is estimated by $52.43kg$ with the maximum overall energy efficiency of 24.36% in peak time. Furthermore, considering $2700hr$ sunshine per year with average DNI of 1538 $kWhr/m^2$, hydrogen production in this site is estimated by 4.987 tons annually.

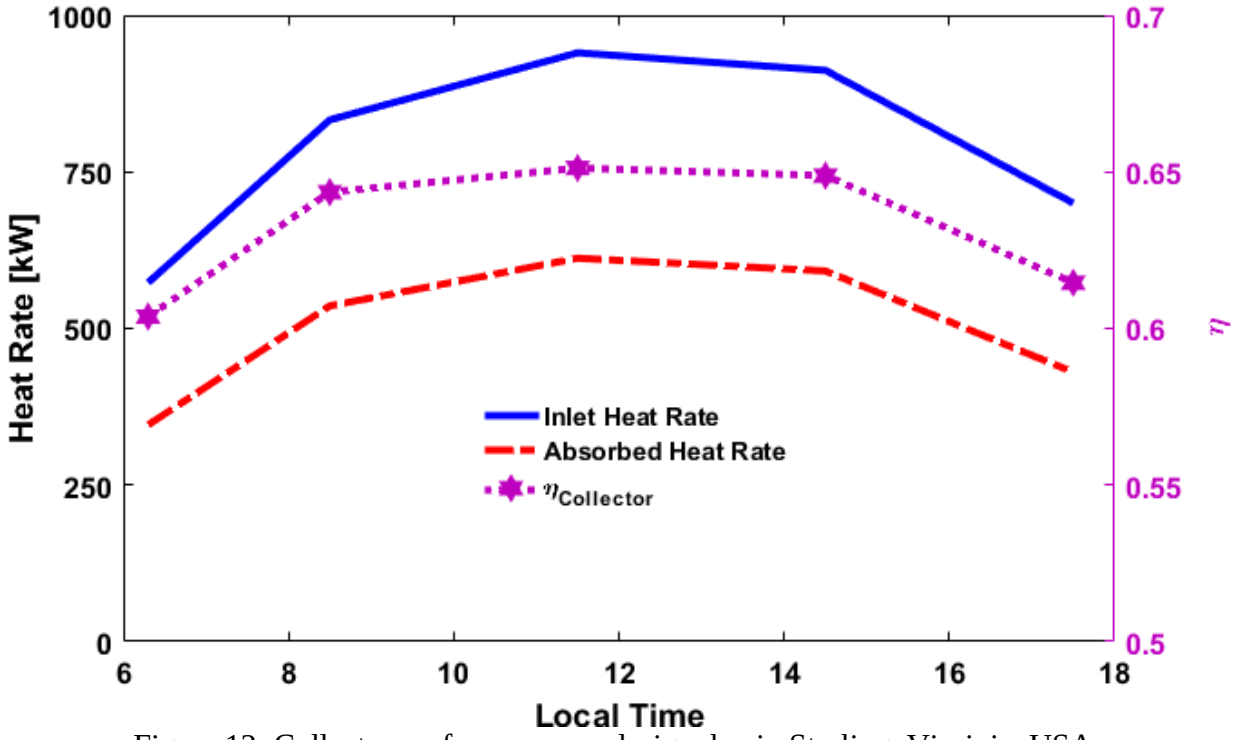

Figure 12: Collector performance on design day in Sterling, Virginia, USA

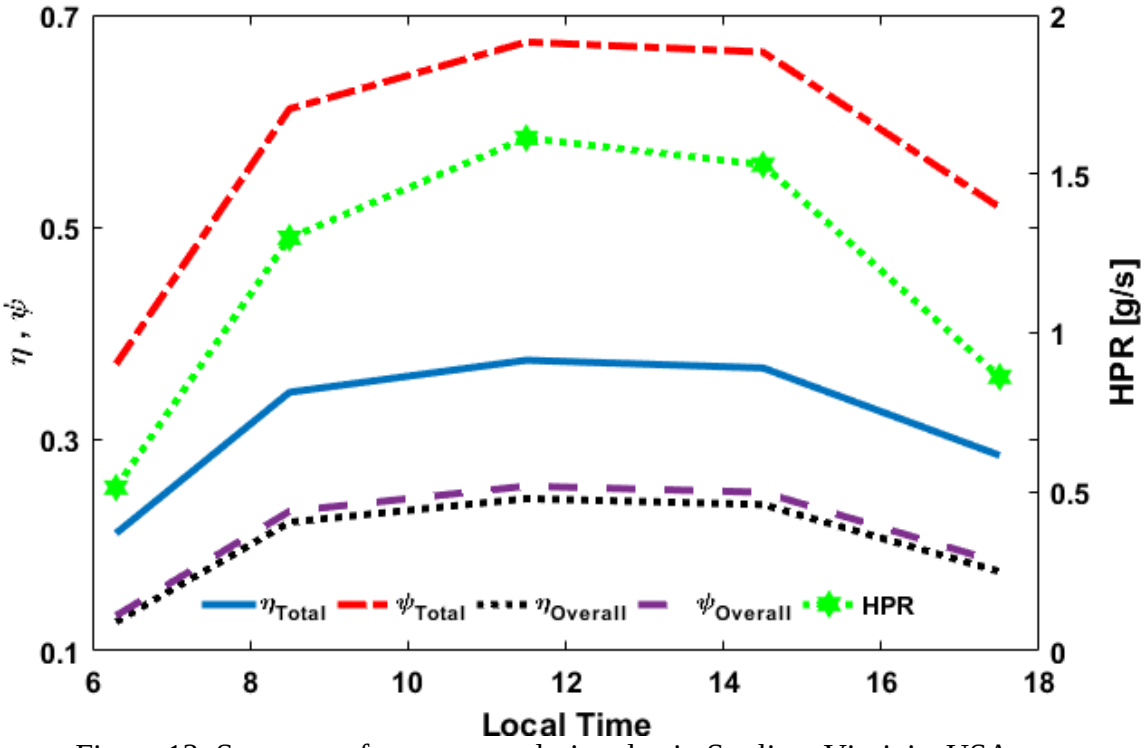

Figure 13: System performance on design day in Sterling, Virginia, USA

Case2:

The other site for a case study is Babol Noshirvani University of Technology, Babol, Iran, with the latitude of 36.56 and longitude of 52.68. The solar data of this site is adopted from ref [66], and the inlet parameters variations during the design day are shown in Fig. 14.

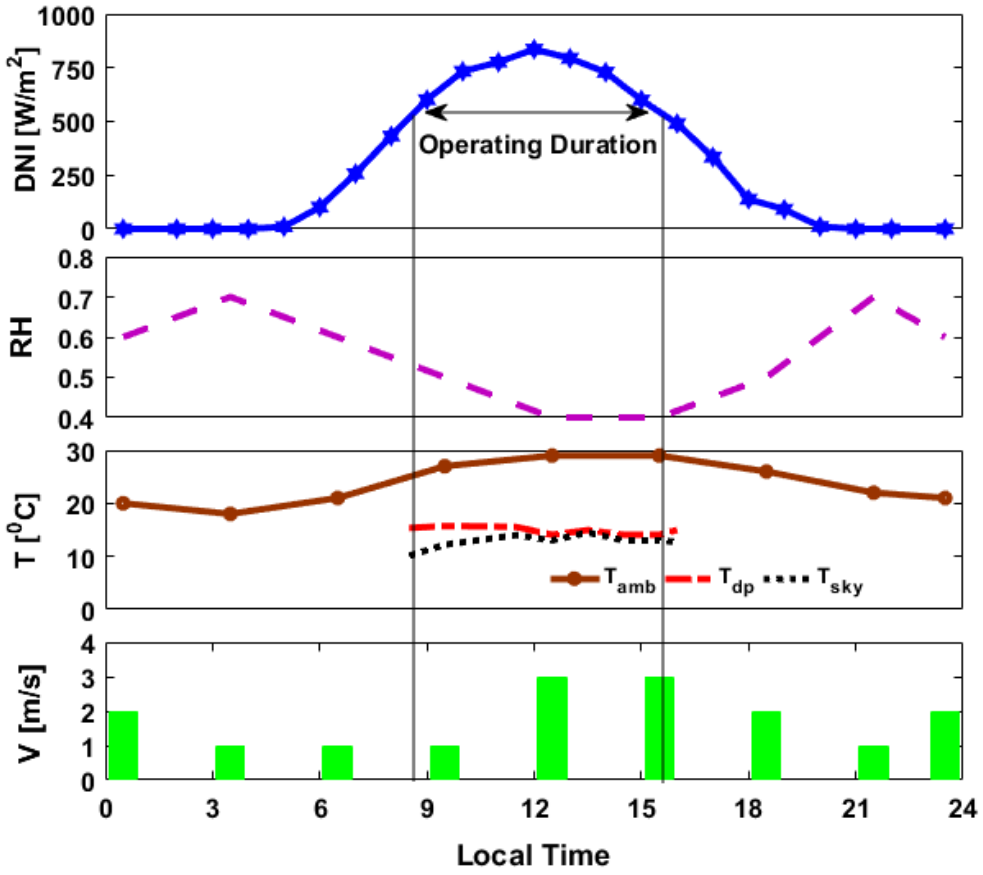

Figure 14: The variation of solar irradiance and weather condition in NIT, Babol, Iran on 15/06/2018

The proposed system can be run for almost 7.5hr at NIT site as it is shown in Fig. 14. The range of collector efficiency variation during the run time is the same of the Sterling site while the peak time of inlet heat flux from the sun is occurred at 12:30pm, local time that is shown in Fig. 15. Peak hydrogen production rate is also estimated by 1.3g/s reported in Fig. 16. Generally, the potential of hydrogen production at NIT site on the design day is estimated by 26.45kg with the maximum overall energy efficiency of 22.09% in peak time. Furthermore, considering 2034hr sunshine per year with average DNI of 1174 $kWhr/m$^2, hydrogen production in this site is estimated by 3.935 tons annually.

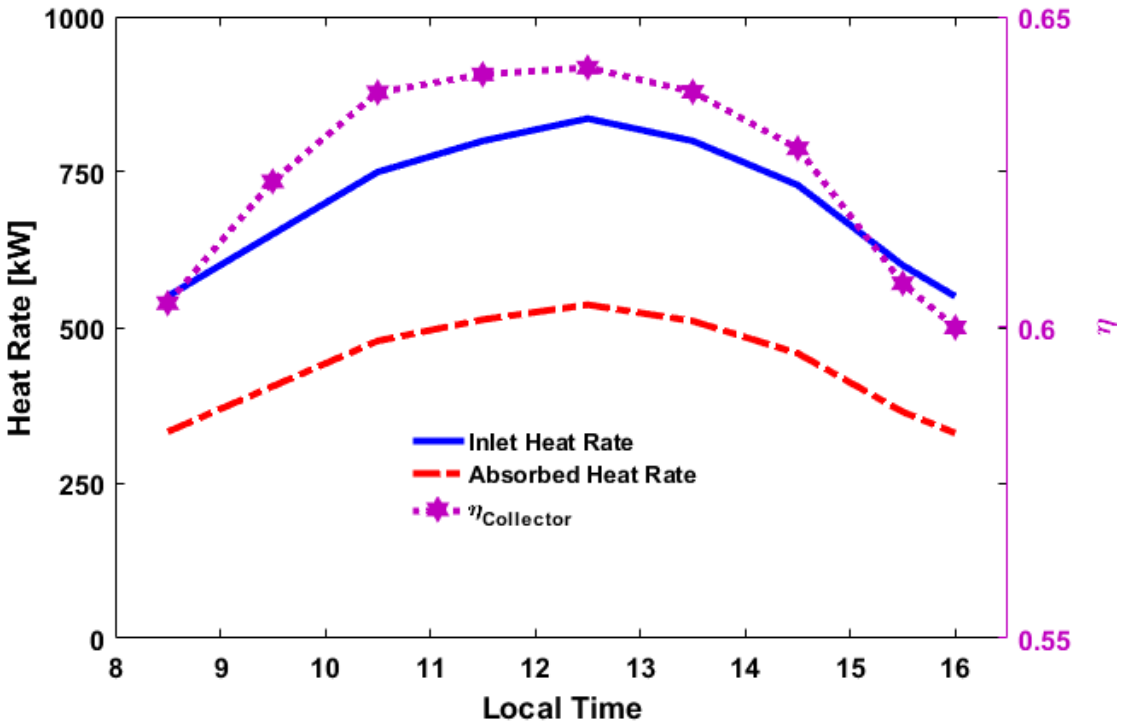

Figure 15: Collector performance on design day in NIT, Babol, Iran

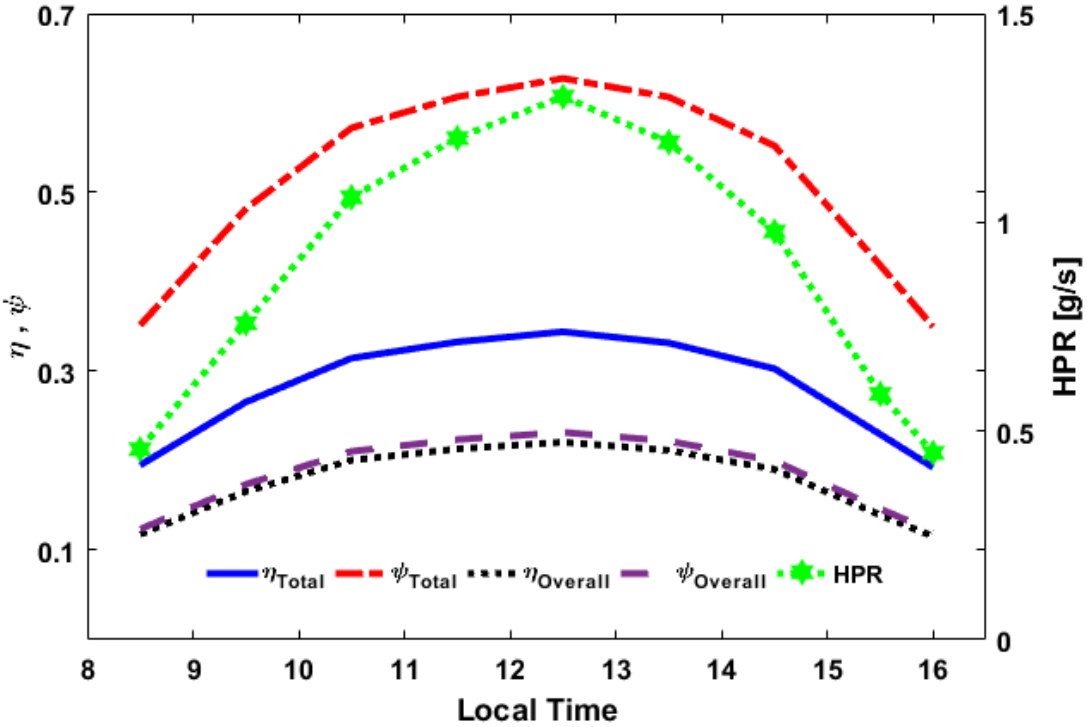

Figure 16: System performance on design day in NIT, Babol, Iran

5. Conclusion:

In this study, a conceptual design of a solar-driven high-temperature steam electrolyzer system is provided, and its performance is investigated thermodynamically. The parametric study of inlet parameters on the system performance is performed, and the real-time system operation on the design day at two different sites is calculated. The main results of the study are listed in the following;

- The proposed system is able to separate 98% of hydrogen from the feed water and produce pure hydrogen with the rate of $1.2 g/s$.
- Overall energy and exergy efficiencies of the designed system are calculated 21.5% and 22.5%, respectively.
- The main inlet exergy destruction occurs in solar collectors, which is 36.4%.
- Direct normal irradiance and incidence angle are the main effective parameters on the heat absorption while relative humidity has no significant effect.
- Designed system has 24.36% overall energy efficiency and produced 52.43kg hydrogen on the design day at Sterling site during its 12hr run time.
- Designed system has 22.09% overall energy efficiency and produced 26.45kg hydrogen on the design day at NIT site during its 7.5hr run time.

Acknowledgment:

This study is partially supported by the Fujian Province Natural Science Foundation (No: 2018J01506), University-industry cooperation program of Department of Science and Technology of Fujian Province (No.2019H6018), Fuzhou Science and Technology Planning Project (No: 2018S113,2018G92), Educational Research Projects of Young Teachers of Fujian Province

(No.JK2017038,JAT170439), 2017 Outstanding Young Scientist Training Program of Colleges in Fujian Province, and Australia ARC DECRA (No. DE190100931).

References:

[1] M.S. Shadloo, R. Poultangari, M.Y. Abdollahzadeh Jamalabadi, M.M. Rashidi, A new and efficient mechanism for spark ignition engines, Energy conversion and management, 96 (2015) 418-429.

[2] R. Alamian, R. Shafaghat, M.R. Safaei, Multi-objective optimization of a pitch point absorber wave energy converter, Water, 11 (2019) 969.

[3] M.Y. Abdollahzadeh Jamalabadi, M. Ghasemi, R. Alamian, E. Afshari, S. Wongwises, M. Mehdi Rashidi, M. Safdari Shadloo, A 3D simulation of single-channel high-temperature polymer exchange membrane fuel cell performances, Applied Sciences, 9 (2019) 3633.

[4] S.A. Atyabi, E. Afshari, S. Wongwises, W.-M. Yan, A. Hadjadj, M.S. Shadloo, Effects of assembly pressure on PEM fuel cell performance by taking into accounts electrical and thermal contact resistances, Energy, 179 (2019) 490-501.

[5] S. Toghyani, S. Fakhradini, E. Afshari, E. Baniasadi, M.Y.A. Jamalabadi, M.S. Shadloo, Optimization of operating parameters of a polymer exchange membrane electrolyzer, International Journal of Hydrogen Energy, 44 (2019) 6403-6414.

[6] R. Alamian, R. Shafaghat, R. Bayani, A.H. Amouei, An experimental evaluation of the effects of sea depth, wave energy converter's draft and position of centre of gravity on the performance of a point absorber wave energy converter, Journal of Marine Engineering & Technology, 16 (2017) 70-83.

[7] R. Alamian, R. Shafaghat, M.S. Shadloo, R. Bayani, A.H. Amouei, An empirical evaluation of the sea depth effects for various wave characteristics on the performance of a point absorber wave energy converter, Ocean Engineering, 137 (2017) 13-21.

[8] H.A. Amiri, R. Shafaghat, R. Alamian, S.M. Taheri, M.S. Shadloo, Study of horizontal axis tidal turbine performance and investigation on the optimum fixed pitch angle using CFD, International Journal of Numerical Methods for Heat & Fluid Flow, 30 (2019) 206-227.

[9] M. Ebrahimpour, R. Shafaghat, R. Alamian, M. Safdari Shadloo, Numerical Investigation of the Savonius Vertical Axis Wind Turbine and Evaluation of the Effect of the Overlap Parameter in Both Horizontal and Vertical Directions on Its Performance, Symmetry, 11 (2019) 821.
[10] S. Toghyani, E. Afshari, E. Baniasadi, M. Shadloo, Energy and exergy analyses of a nanofluid based solar cooling and hydrogen production combined system, Renewable energy, 141 (2019) 1013-1025.
[11] C. Yilmaz, M. Kanoglu, Thermodynamic evaluation of geothermal energy powered hydrogen production by PEM water electrolysis, Energy, 69 (2014) 592-602.
[12] C. Yilmaz, M. Kanoglu, A. Abusoglu, Thermoeconomic cost evaluation of hydrogen production driven by binary geothermal power plant, Geothermics, 57 (2015) 18-25.
[13] A. Maleki, Modeling and optimum design of an off-grid PV/WT/FC/diesel hybrid system considering different fuel prices, International Journal of Low-Carbon Technologies, 13 (2018) 140-147.
[14] A. Maleki, H. Hafeznia, M.A. Rosen, F. Pourfayaz, Optimization of a grid-connected hybrid solar-wind-hydrogen CHP system for residential applications by efficient metaheuristic approaches, Applied Thermal Engineering, 123 (2017) 1263-1277.
[15] A. Maleki, M.A. Rosen, Design of a cost-effective on-grid hybrid wind–hydrogen based CHP system using a modified heuristic approach, International Journal of Hydrogen Energy, 42 (2017) 15973-15989.
[16] W. Zhang, A. Maleki, M.A. Rosen, J. Liu, Sizing a stand-alone solar-wind-hydrogen energy system using weather forecasting and a hybrid search optimization algorithm, Energy conversion and management, 180 (2019) 609-621.
[17] S.P. Zanous, R. Shafaghat, R. Alamian, M.S. Shadloo, M. Khosravi, Feasibility study of wave energy harvesting along the southern coast and islands of Iran, Renewable energy, 135 (2019) 502-514.
[18] M.M. Namar, O. Jahanian, Energy and exergy analysis of a hydrogen-fueled HCCI engine, Journal of Thermal Analysis and Calorimetry, 137 (2019) 205-215.
[19] A. Rimkus, J. Matijošius, M. Bogdevičius, Á. Bereczky, Á. Török, An investigation of the efficiency of using O2 and H2 (hydrooxile gas-HHO) gas additives in a CI engine operating on diesel fuel and biodiesel, Energy, 152 (2018) 640-651.

[20] A. Sánchez, M. Martin, Optimal renewable production of ammonia from water and air, Journal of Cleaner Production, 178 (2018) 325-342.
[21] C. Acar, I. Dincer, A review and evaluation of photoelectrode coating materials and methods for photoelectrochemical hydrogen production, International Journal of Hydrogen Energy, 41 (2016) 7950-7959.
[22] M.T. Balta, O. Kizilkan, F. Yılmaz, Energy and exergy analyses of integrated hydrogen production system using high temperature steam electrolysis, International Journal of Hydrogen Energy, 41 (2016) 8032-8041.
[23] A. Kazim, Hydrogen production through an ocean thermal energy conversion system operating at an optimum temperature drop, Applied Thermal Engineering, 25 (2005) 2236-2246.
[24] Y. Li, H. Chen, X. Zhang, C. Tan, Y. Ding, Renewable energy carriers: Hydrogen or liquid air/nitrogen?, Applied Thermal Engineering, 30 (2010) 1985-1990.
[25] A. Modarresi, W. Wukovits, A. Friedl, Application of exergy balances for evaluation of process configurations for biological hydrogen production, Applied Thermal Engineering, 30 (2010) 70-76.
[26] S.S. Murthy, E.A. Kumar, Advanced materials for solid state hydrogen storage:"Thermal engineering issues", Applied Thermal Engineering, 72 (2014) 176-189.
[27] P.A. Pilavachi, S.D. Stephanidis, V.A. Pappas, N.H. Afgan, Multi-criteria evaluation of hydrogen and natural gas fuelled power plant technologies, Applied Thermal Engineering, 29 (2009) 2228-2234.
[28] O. Siddiqui, H. Ishaq, I. Dincer, A novel solar and geothermal-based trigeneration system for electricity generation, hydrogen production and cooling, Energy conversion and management, 198 (2019) 111812.
[29] E. Akrami, I. Khazaee, A. Gholami, Comprehensive analysis of a multi-generation energy system by using an energy-exergy methodology for hot water, cooling, power and hydrogen production, Applied Thermal Engineering, 129 (2018) 995-1001.
[30] P. Bartocci, M. Zampilli, G. Bidini, F. Fantozzi, Hydrogen-rich gas production through steam gasification of charcoal pellet, Applied Thermal Engineering, 132 (2018) 817-823.
[31] M. Ozturk, I. Dincer, Thermodynamic analysis of a solar-based multi-generation system with hydrogen production, Applied Thermal Engineering, 51 (2013) 1235-1244.

[32] T.A.H. Ratlamwala, I. Dincer, Comparative efficiency assessment of novel multi-flash integrated geothermal systems for power and hydrogen production, Applied Thermal Engineering, 48 (2012) 359-366.
[33] A. Bilodeau, K. Agbossou, Control analysis of renewable energy system with hydrogen storage for residential applications, Journal of power sources, 162 (2006) 757-764.
[34] M. Nouri, M.M. Namar, O. Jahanian, Analysis of a developed Brayton cycled CHP system using ORC and CAES based on first and second law of thermodynamics, Journal of Thermal Analysis and Calorimetry, 135 (2019) 1743-1752.
[35] B. Yildiz, M.S. Kazimi, Efficiency of hydrogen production systems using alternative nuclear energy technologies, International Journal of Hydrogen Energy, 31 (2006) 77-92.
[36] M. Kanoglu, A. Bolatturk, C. Yilmaz, Thermodynamic analysis of models used in hydrogen production by geothermal energy, International Journal of Hydrogen Energy, 35 (2010) 8783-8791.
[37] M. Kanoglu, C. Yilmaz, A. Abusoglu, Geothermal Energy Use in Hydrogen Production, Journal of Thermal Engineering, 2 (2016) 699-708.
[38] J. Sigurvinsson, C. Mansilla, P. Lovera, F. Werkoff, Can high temperature steam electrolysis function with geothermal heat?, International Journal of Hydrogen Energy, 32 (2007) 1174-1182.
[39] C. Yilmaz, M. Kanoglu, A. Abusoglu, Exergetic cost evaluation of hydrogen production powered by combined flash-binary geothermal power plant, International Journal of Hydrogen Energy, 40 (2015) 14021-14030.
[40] A. Demin, E. Gorbova, P. Tsiakaras, High temperature electrolyzer based on solid oxide co-ionic electrolyte: A theoretical model, Journal of power sources, 171 (2007) 205-211.
[41] H. Ishaq, I. Dincer, Design and performance evaluation of a new biomass and solar based combined system with thermochemical hydrogen production, Energy conversion and management, 196 (2019) 395-409.
[42] I. Dincer, C. Acar, Review and evaluation of hydrogen production methods for better sustainability, International Journal of Hydrogen Energy, 40 (2015) 11094-11111.
[43] H. Zhang, S. Su, X. Chen, G. Lin, J. Chen, Configuration design and performance optimum analysis of a solar-driven high temperature steam electrolysis system for hydrogen production, International Journal of Hydrogen Energy, 38 (2013) 4298-4307.

[44] L. Mingyi, Y. Bo, X. Jingming, C. Jing, Thermodynamic analysis of the efficiency of high-temperature steam electrolysis system for hydrogen production, Journal of power sources, 177 (2008) 493-499.
[45] J.S. Herring, J.E. O'Brien, C.M. Stoots, G. Hawkes, J.J. Hartvigsen, M. Shahnam, Progress in high-temperature electrolysis for hydrogen production using planar SOFC technology, International Journal of Hydrogen Energy, 32 (2007) 440-450.
[46] J.S. Kim, R.D. Boardman, S.M. Bragg-Sitton, Dynamic performance analysis of a high-temperature steam electrolysis plant integrated within nuclear-renewable hybrid energy systems, Applied energy, 228 (2018) 2090-2110.
[47] D. Yadav, R. Banerjee, Economic assessment of hydrogen production from solar driven high-temperature steam electrolysis process, Journal of Cleaner Production, 183 (2018) 1131-1155.
[48] S.S. Kaleibari, Z. Yanping, S. Abanades, Solar-driven high temperature hydrogen production via integrated spectrally split concentrated photovoltaics (SSCPV) and solar power tower, International Journal of Hydrogen Energy, 44 (2019) 2519-2532.
[49] F.M. Nafchi, E. Baniasadi, E. Afshari, N. Javani, Performance assessment of a solar hydrogen and electricity production plant using high temperature PEM electrolyzer and energy storage, International Journal of Hydrogen Energy, 43 (2018) 5820-5831.
[50] E. Akyuz, C. Coskun, Z. Oktay, I. Dincer, Hydrogen production probability distributions for a PV-electrolyser system, International Journal of Hydrogen Energy, 36 (2011) 11292-11299.
[51] C. Coskun, Z. Oktay, An Advanced Simple Method for Generating Synthetic Average instant Hourly Solar energy, Journal of Management Science & Engineering Research, 01 (2018) 1-6.
[52] Z. Oktay, C. Coskun, I. Dincer, A new approach for predicting cooling degree-hours and energy requirements in buildings, Energy, 36 (2011) 4855-4863.
[53] A. Habibollahzade, E. Gholamian, P. Ahmadi, A. Behzadi, Multi-criteria optimization of an integrated energy system with thermoelectric generator, parabolic trough solar collector and electrolysis for hydrogen production, International Journal of Hydrogen Energy, 43 (2018) 14140-14157.
[54] S.S. Sabet, M. Namar, M. Sheikholeslami, A. Shafee, Thermodynamics analysis for high temperature hydrogen production system, Scientia Iranica, (2019).
[55] S. Odeh, G. Morrison, M. Behnia, Modelling of parabolic trough direct steam generation solar collectors, Solar energy, 62 (1998) 395-406.

[56] V. Dudley, G. Kolb, M. Sloan, D. Kearney, SEGS LS2 solar collector-test results, Report of Sandia National Laboratories, Report No. SANDIA94-1884, (1994).
[57] M. Martin, P. Berdahl, Characteristics of infrared sky radiation in the United States, Solar energy, 33 (1984) 321-336.
[58] R.E. Sonntag, C. Borgnakke, G.J. Van Wylen, S. Van Wyk, Fundamentals of thermodynamics, Wiley New York, 1998.
[59] M.T. Balta, I. Dincer, A. Hepbasli, Thermodynamic assessment of geothermal energy use in hydrogen production, International Journal of Hydrogen Energy, 34 (2009) 2925-2939.
[60] National Institute of Standards and Technology (NIST), June 2005. Availabe online: http://webbook.nist.gov/chemistry/ (accessed on August 6, 2019). in, Vol. 2019.
[61] The Exergoecology Portal, 2008. Availabe online: http://www.exergoecology.com/excalc/ (accessed on August 6, 2019). in.
[62] F. Yilmaz, M. Ozturk, R. Selbas, Energy and exergy performance assessment of a novel solar-based integrated system with hydrogen production, International Journal of Hydrogen Energy, 44 (2019) 18732-18743.
[63] C. Coskun, U. Toygar, O. Sarpdag, Z. Oktay, Sensitivity analysis of implicit correlations for photovoltaic module temperature: A review, Journal of Cleaner Production, 164 (2017) 1474-1485.
[64] Ventusky web application. Availabe online: https://www.ventusky.com (accessed on August 6, 2019). in.
[65] Earth System Research Laboratory, Global Monitoring Division. Availabe online: https://www.esrl.noaa.gov/gmd/grad/solrad/solradpick.html (accessed on August 6, 2019). in.
[66] Solargis s.r.o., Mytna 48, 811 07 Bratislava, Slovakia. Availabe online: http://solargis.com (accessed on August 6, 2019). in.

Appendix

The simulator geraphical description

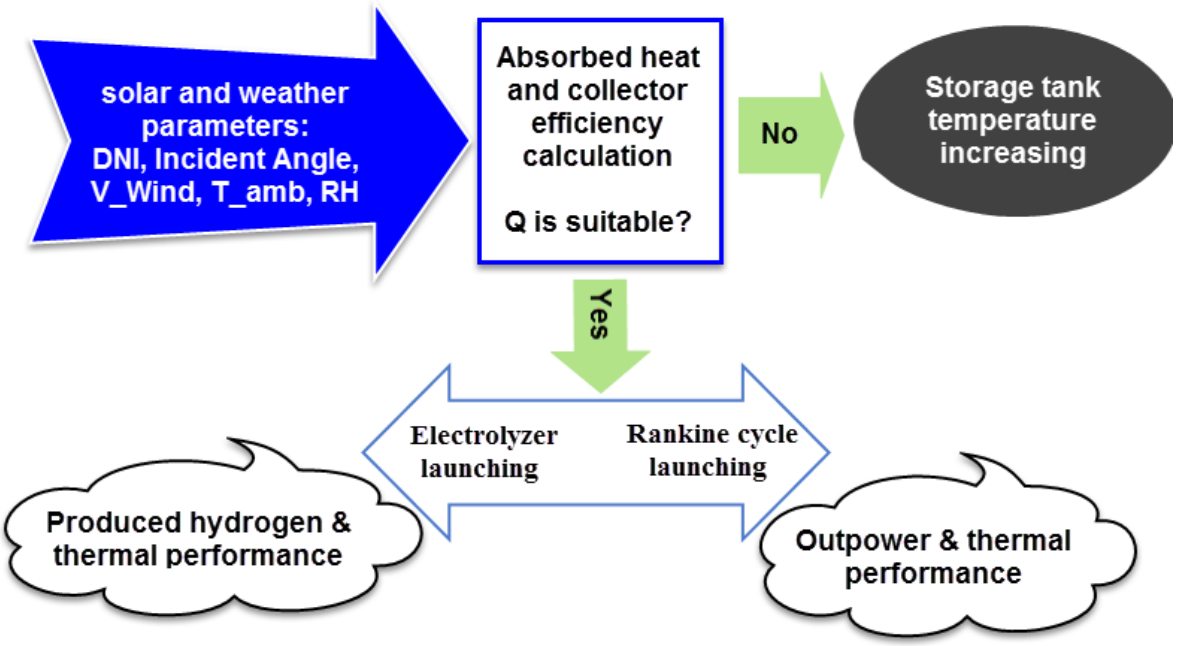
solar and weather parameters:
DNI, Incident Angle, V_Wind, T_amb, RH
Absorbed heat and collector efficiency calculation
Q is suitable?
No
Storage tank temperature increasing
Yes
Electrolyzer launching
Rankine cycle launching
Produced hydrogen & thermal performance
Outpower & thermal performance